Electronic Supplementary Material (ESI) for Nanoscale.

Supporting information

Local Electrochemical Activity of Transition Metal Dichalcogenides and Their Heterojunctions on 3D-Printed Nanocarbon Surfaces

Katarina A. Novčić[a], Christian Iffelsberger[a], Siowwoon Ng[a] and Martin Pumera[a,b,c,d*]

[a]Future Energy and Innovation Laboratory, Central European Institute of Technology, Brno University of Technology, Purkyňova 123, 61200 Brno, Czech Republic.

[b]Department of Chemistry and Biochemistry, Mendel University in Brno, Zemedelska 1, CZ-613 00, Brno, Czech Republic

[c]Department of Chemical and Biomolecular Engineering, Yonsei University, 50 Yonsei-ro, Seodaemun-gu, Seoul 03722, Korea.

[d]Department of Medical Research, China Medical University Hospital, China Medical University, No. 91 Hsueh Road, Taichung 40402, Taiwan.

*E-mail: pumera.research@gmail.com

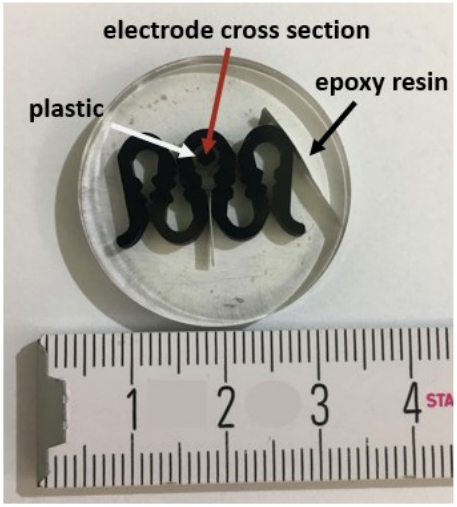

Figure S1: Photograph of the prepared sample cross section for the SECM measurement (scale is in cm).

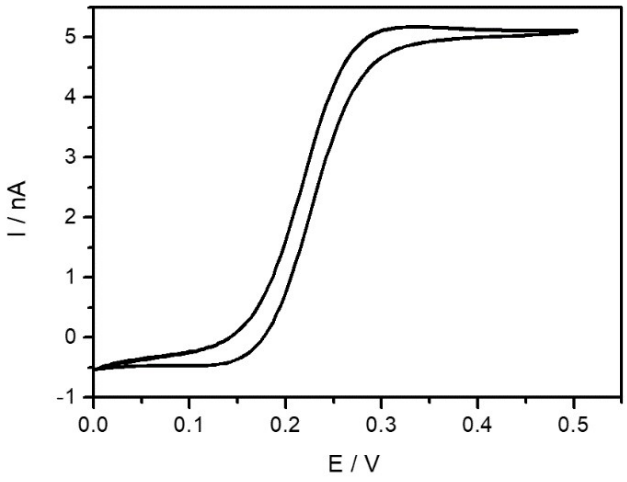

Figure S2: Cyclic volatmmetry of 25 µm diameter UME tip probe. Measurement was performed in 1.5 mM FcMeOH and 0.2 M KNO_3 mediator solution. Conditions: a scan rate of 50 mV s^{-1}, potential range from 0 V to 0.5 V, starting from open circuit potential.

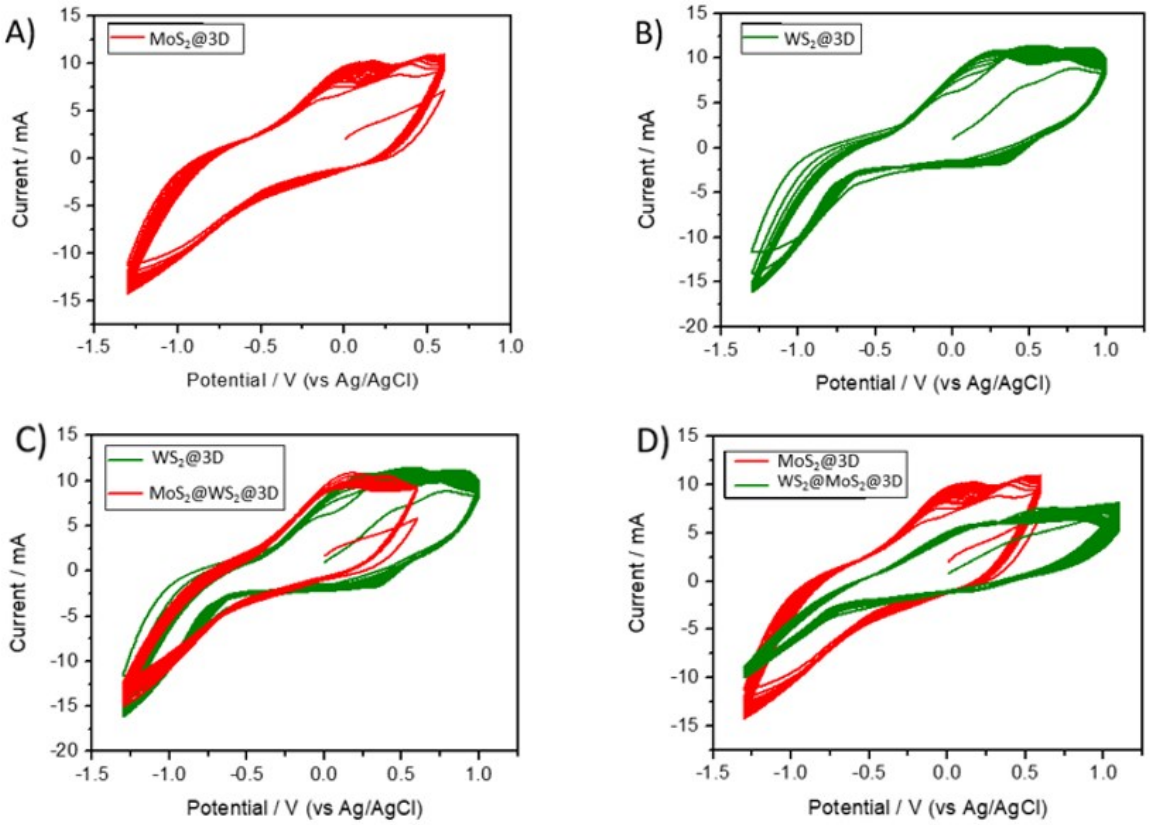

Figure S3: Cyclic voltammograms of electrochemical deposition for MoS_2@3D (A), WS_2@3D (B), WS_2@3D (green curve) and MoS_2@WS_2@3D (red curve) (C), MoS_2@3D (red curve) and WS_2@MoS_2@3D (green curve) electrodes (D).

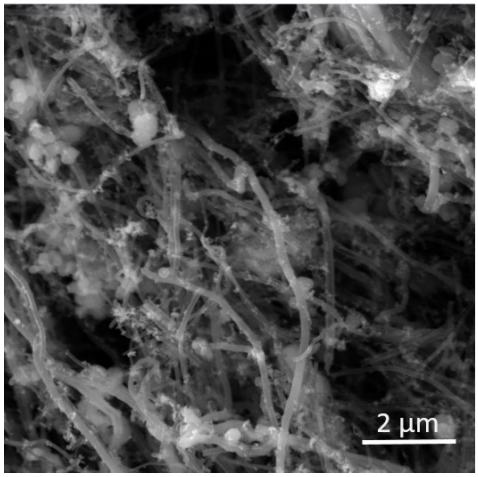

Figure S4: SEM micrograph of the thermally activated 3D-printed electrode.

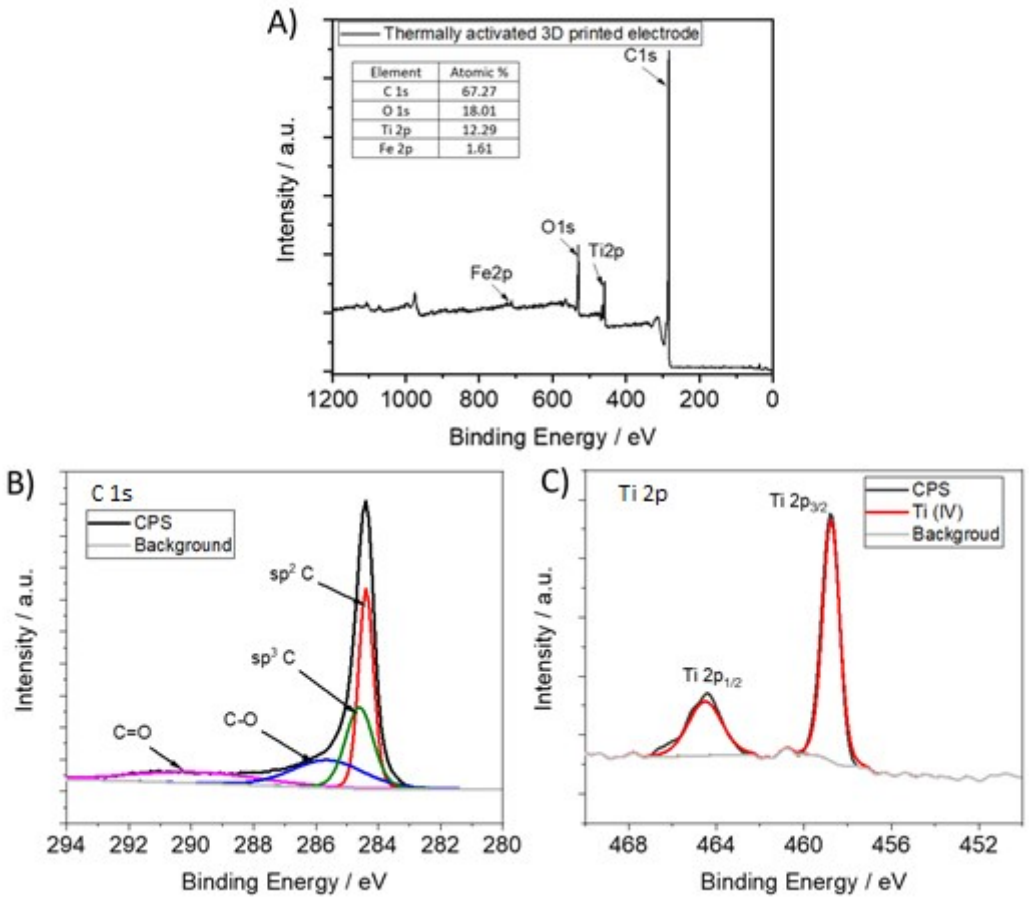

Figure S5: X-ray photoelectron spectroscopy study of the thermally activated 3D-printed electrode, survey spectra (A) and deconvolution of C1s (B), and Ti 2p (C).

X-ray photoelectron spectroscopy of thermally activated 3D-printed electrode surface:

The XPS survey spectrum of thermally activated 3D-printed electrodes is presented in Figure S5 A and confirms the presence of C, O, Ti and Fe on the electrode surface. The deconvolution of the C 1s (Figure S5 B) spectrum confirms the presence of carbon C=C sp^2 bond and other carbon functional groups such as C-O, C=O in the carbon-based filament. Moreover, the deconvolution of the Ti 2p spectrum (Figure S5 C) indicates the presence of Ti (IV) $2p_{1/2}$ and Ti (IV) $2p_{3/2}$ states observed at 464.5 eV and 458.7 eV, respectively, which points on the presence of TiO_2 and it is in line with the literature[1-3].

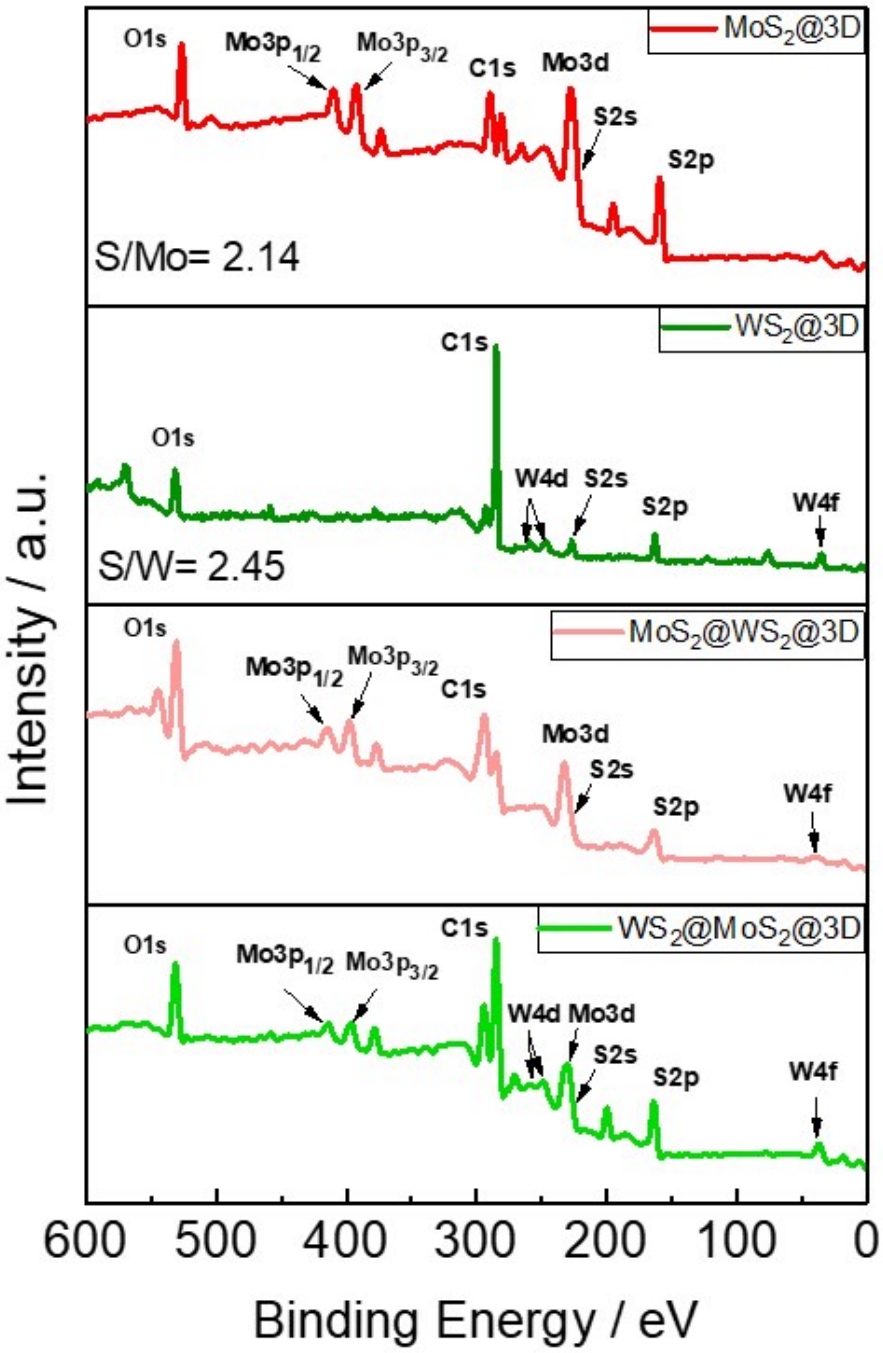

Figure S6: X-ray photoelectron spectroscopy study of the TMD modified thermally activated 3D-printed electrodes. Insets in the XPS survey spectrum for MoS_2@3D and WS_2@3D samples show the ratio between S and Mo (S/Mo) and S and W (S/W), respectively.

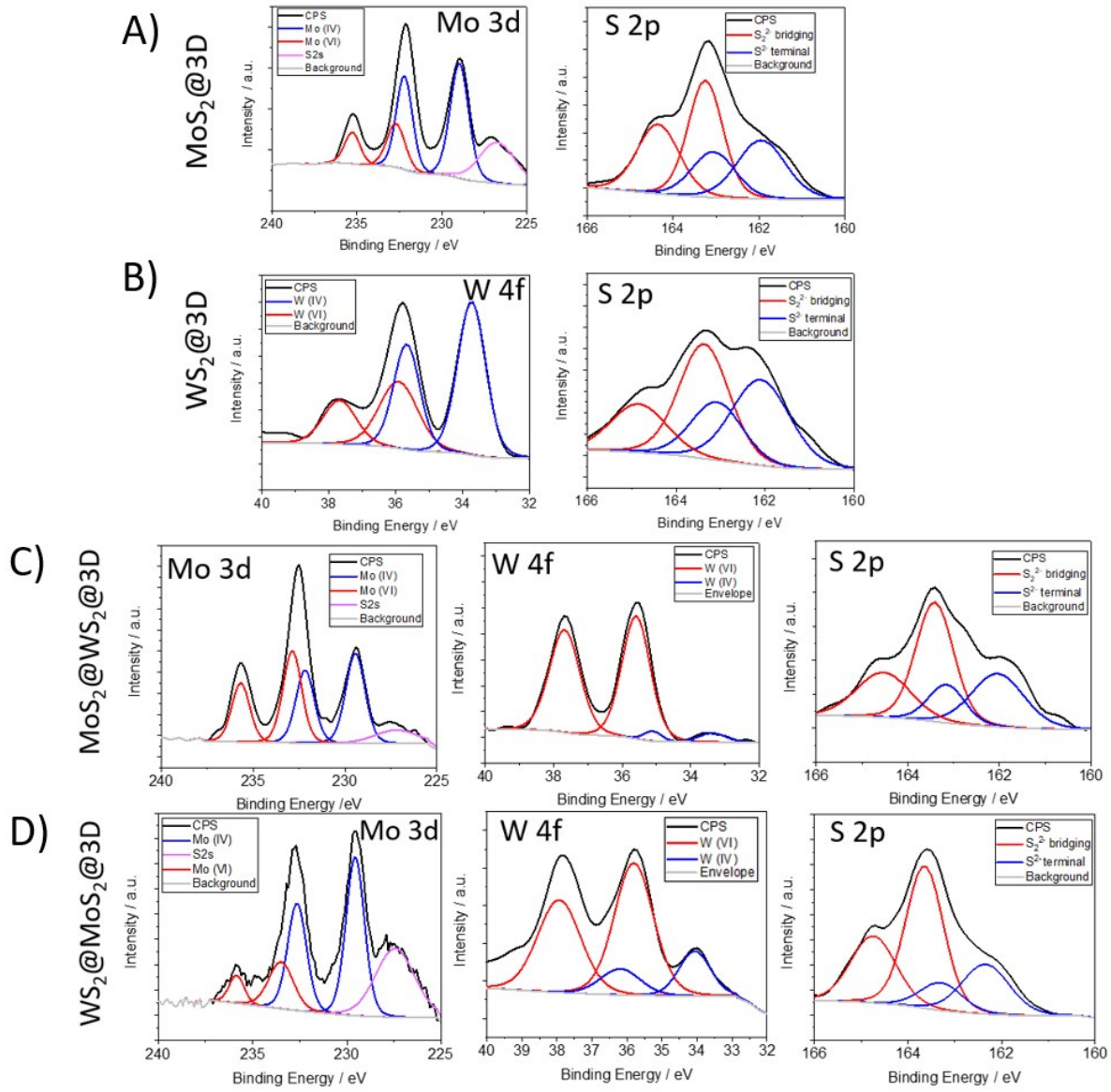

Figure S7: X-ray photoelectron spectroscopy study of the specific element deconvolutions for Mo 3d, W 4f and S 2p for the MoS_2@3D (A), WS_2@3D (B), MoS_2@WS_2@3D (C) and WS_2@MoS_2@3D (D) electrodes.

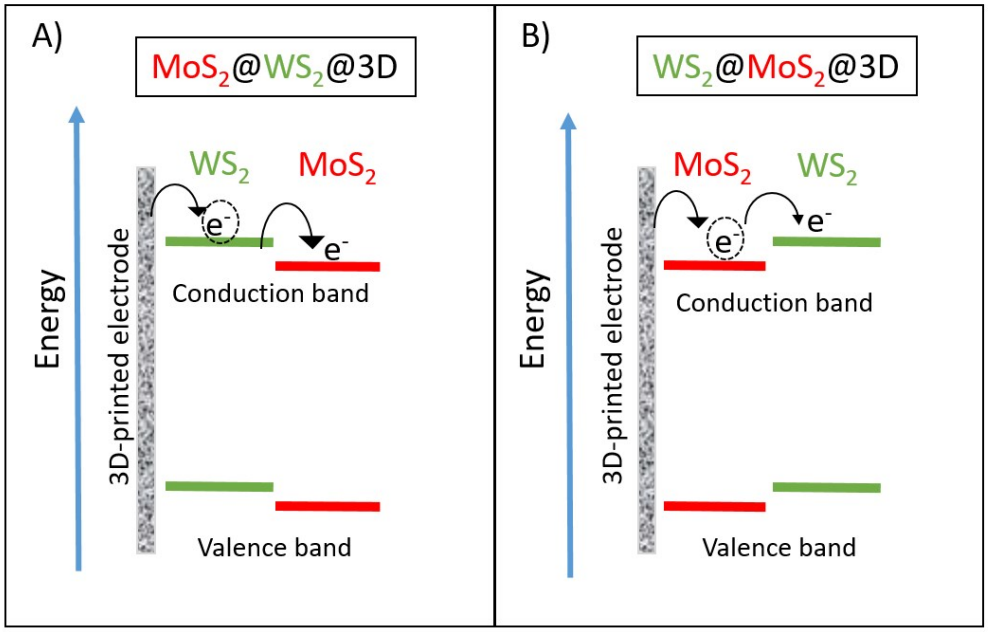

Scheme S1: Schematic energy band diagrams for MoS_2 and WS_2 in MoS_2@WS_2@3D (A) and WS_2@MoS_2@3D (B) electrodes. Band positions are estimated based on the literature[4-6].

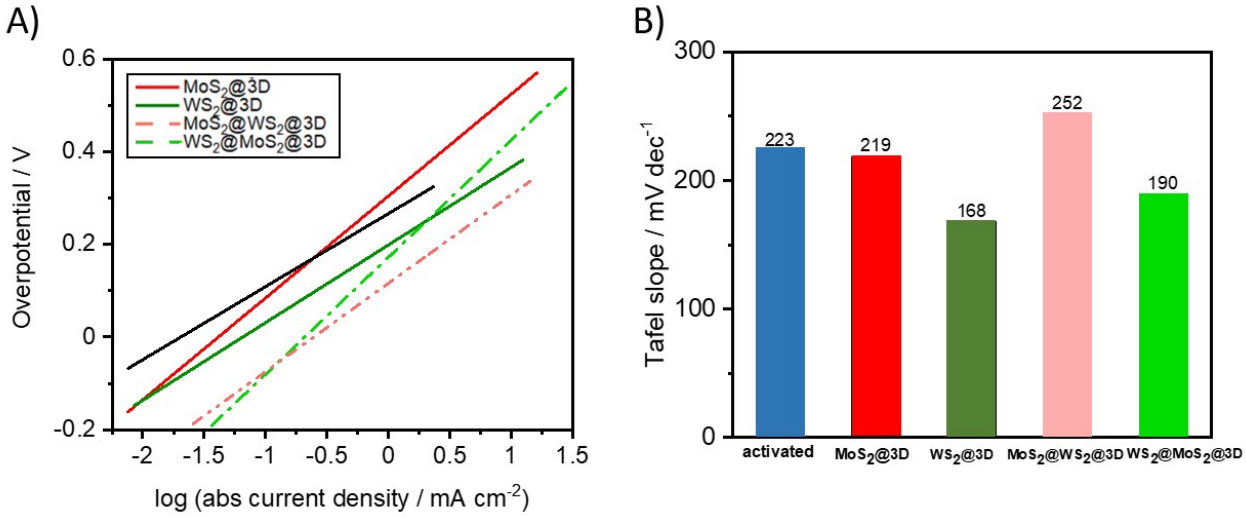

Figure S8: Tafel plots calculated from LSV measurements (A) and bar charts comparing the calculated Tafel slope values (B).

Table S1: Comparison of the active catalysts supported by 3D-printed platform for hydrogen evolution reaction.

Catalyst	Electrolyte	HER overpotential at -10 mA cm^{-2} (V vs RHE)	Tafel slope / mV dec^{1}	Ref.
Ni-modified 3D-steel	1M KOH	- 0.40	131	[7]
MoS_2-modified-3D-steel	1M KOH	- 0.35	120	[7]
Ni-MoS_2-modified-3D-steel	1M KOH	- 0.30	106	[7]
$NiCo_2S_4$-spray coated 3D	0.5M H_2SO_4	- 0.226	38.7	[8]
ReS_2@3D*	0.5 M H_2SO_4	- 0.28	147	[9]
MoS_2 spray coated 3D	0.5 M H_2SO_4	~- 0.55	N/A**	[10]
$MoS_{3-\delta}$@3D	0.5 M H_2SO_4	- 0.298	119	[11]
MoS_2@3D	0.5 M H_2SO_4	- 0.28	220	this work
WS_2@3D	0.5 M H_2SO_4	- 0.53	168	this work
MoS_2@WS_2@3D	0.5 M H_2SO_4	- 0.32	152	this work
WS_2@MoS_2@3D	0.5 M H_2SO_4	- 0.43	190	this work

*3D - 3D-printed electrode; ** N/A – not available

References:

1. S. Yang, Y. Lin, X. Song, P. Zhang, L. Gao, *ACS Appl. Mater. Interfaces 2015, 7, 32, 17884-17892*.

1. S. Yang, Y. Lin, X. Song, P. Zhang, L. Gao, ACS Appl. Mater. Interfaces 2015, 7, 32, 17884-17892.

2. K. Ghosh, S. Ng, C. Iffelsberger, M. Pumera, *Chem. Eur. J. 2020, 26, 67, 15746-15753*.

3. M. P. Browne, V. Urbanova, J. Plutnar, F. Novotny, M. Pumera, *J. Mater. Chem. A 2020, 8, 1120-1126.*

4. V. Kaushik, M. Ahmad, K. Agarwal, D. Varandani, B.D. Belle, P. Das, B.R. Mehta, *J. Phys. Chem.C. 2020, 124, 23368-23379.*

5. L. Li, R. Long, O.V. Prezhdo, *Chem. Mater. 2017, 29, 2466-2473.*

6. Y. Liang, S. Huang, R. Soklaski, L. Yang, *Appl. Phys. Lett, 2013, 103, 042106.*

7. A. Ambrosi, M. Pumera, *ACS Sustain. Chem. Eng. 2018, 6, 12, 16968-16975*.

8. S. Chang, X. Huang, C.Y.A. Ong, L. Zhao, L. Li, X. Wang, J. Ding, *J. Mater. Chem. A, 2019, 7, 18338-18347.*

9. S. Ng, C. Iffelsberger, Z. Sofer, M. Pumera, *Adv. Funct. Mater. 2020, 30, 1910193*.

10. R. Gusmao, Z. Sofer, P. Marvan, M. Pumera, *Nanoscale 2019, 11, 9888-9895.*

11. C. Iffelsberger, S. Ng, M. Pumera, *Appl. Mater. Today 2020, 20, 100654*.